1994ApJ...436L..51F

Fe K EMISSION FROM THE HIDDEN QUASAR IRAS P09104+4109

A. C. FABIAN,[1] Y. SHIOYA,[2] K. IWASAWA,[3] K. NANDRA,[1] C. CRAWFORD,[1] R. JOHNSTONE,[1] H. KUNIEDA,[3]
R. McMAHON, K. MAKISHIMA,[4] T. MURAYAMA,[2] T. OHASHI,[5] Y. TANAKA,[6]
Y. TANIGUCHI,[2] AND Y. TERASHIMA[3]

ABSTRACT

We report the discovery of a strong Fe K line in the *ASCA* spectrum of the infrared-luminous galaxy IRAS P09104+4109 at a redshift $z = 0.442$. It is the most distant Fe K emission line detected so far. The large equivalent width (EW $\sim$ 450 eV) and X-ray continuum spectrum, which has $\Gamma \approx 2.0$ with little absorption, favors a model in which the observed X-rays are scattered into our line of sight from a hidden quasar. Previous work has shown that the source has strong narrow emission lines and a highly polarized continuum in the optical and a strong infrared excess, similar to Seyfert 2 galaxies. The observed X-ray luminosity is $L_X \approx 2 \times 10^{45}$ ergs s^{-1} in the rest frame 2–10 keV band; the large obscuration suggested by the optical and infrared studies implies that the hidden quasar has an intrinsic luminosity of $L_{Bol} = 5 \times 10^{47}$ ergs s^{-1}. Our results indicate that IRAS P09104+4109 is the prototype of a new class of Seyfert 2 nuclei, which emit at quasar luminosities.

Subject headings: galaxies: active — galaxies: individual (IRAS P09104+4109) — X-rays: galaxies

1. INTRODUCTION

Many of the luminous objects in the universe have been observed with *IRAS* to emit most of their energy in the far-infrared band. Strong emission lines and a polarized continuum in the optical have led to the suggestion that the hyperluminous *IRAS* galaxies, such as IRAS P09104+4109 (Kleinmann et al. 1988), IRAS F10214+4724 (Rowan-Robinson et al. 1991; Lawrence et al. 1993), and IRAS F15307+3252 (Cutri et al. 1994), are obscured quasars, possibly with a starburst component. At much lower luminosities, obscured active nuclei are commonly seen in Seyfert 2 galaxies. A thick molecular torus of gas surrounds the active nucleus which appears as a Seyfert 2 when viewed along the symmetry axis and as a Seyfert 1 along the plane of the torus (see Antonucci 1993 and references therein). These hyperluminous *IRAS* galaxies may be the long-sought quasar version of Seyfert 2 galaxies.

In this *Letter* we report the X-ray detection with *ASCA* of the ultraluminous *IRAS* galaxy P09104+4109 which lies at redshift $z = 0.442$. It was discovered by Kleinmann et al. (1988), who found strong, narrow, optical emission lines from the cD host galaxy which lies in the center of a flattened cluster of galaxies. Hines & Wills (1993) later found the continuum to be highly polarized, indicative of light scattered by dust or electrons from some central source. The object is also a radio source (Kleinmann et al. 1988), intermediate in power, spectrum and structure to typical F-R I and II sources (Hines & Wills 1993). P09104+4109 is probably the most luminous object within a redshift of $z \sim 0.5$, being more luminous than both 3C 273 [$z = 0.158$, $L(2–10$ keV$) = 1.5 \times 10^{46}$ ergs s^{-1}; Yaqoob et al. 1994], and the quasar H1821+643 [$z = 0.297$,

$L(2–10$ keV$) = 8 \times 10^{45}$ ergs s^{-1}; Kii et al. 1991] to which it bears some similarity.

The X-ray source is pointlike and luminous. We find a large iron emission line in the X-ray spectrum of P09104+4109 which strongly indicates that we are seeing scattered X-ray emission from a hidden quasar.

2. THE *ASCA* DATA

IRAS P09104+4109 was observed with *ASCA* on 1993 November 12. About 38 ks of useful data were obtained after the raw data set was reduced and cleaned of extraneous events. The X-ray image of the source in the SIS instruments (see Tanaka, Inoue, & Holt 1994 for a brief description of *ASCA* and its instrumentation) clearly shows the Maltese cross structure induced by the foil mirrors which is indicative of a point source. We have quantitatively verified this by comparing slices and radial profiles of the image with those from bright active galaxies observed at a similar position on the detectors. The slices are well fitted by a Lorentzian profile of width $56.3^{+0.9}_{-1.9}$ SIS pixels (each of 1''2) for the Seyfert galaxy NGC 5548 and 57 ± 6 pixels for P09104+4109. For comparison, we note that the cluster of galaxies CL 0016+16, which is at $z = 0.54$ and has a similar luminosity to P09104+4109, has a clearly extended image in the SIS with a diameter of 6'–8' (Furuzawa et al. 1994). We conclude that any cluster emission from P09104+4109 does not dominate the flux.

Background-subtracted spectra of the source were successfully accumulated using both SIS instruments (SIS0 and SIS1) and both GIS instruments (GIS2 and GIS3). The spectra are well fitted by an absorbed power law with a strong iron line ($\Delta\chi^2 = 30$) at about 4.6 keV which we identify with iron Kα emission at the redshift of the object (Fig. 1). Results from the separate detectors are given in Table 1; fitting the detectors jointly gives an intrinsic absorption (redshift-corrected) of $2.4 \pm 0.06 \times 10^{21}$ cm^{-2}, photon index $\Gamma = 1.96 \pm 0.06$, intrinsic line energy of 6.67 ± 0.06 keV, observed line width $\sigma = 70^{+90}_{-70}$ eV, and equivalent width (our frame) of 308^{+90}_{-120} eV with a reduced $\chi^2 = 1.18$ for 491 degrees of freedom.

The energy of the iron line is consistent with that of helium-like iron (Fig. 2). There is no evidence for any line at the

[1] Institute of Astronomy, Madingley Road, Cambridge CB3 0HA, UK.
[2] Astronomical Institute, Tohoku University, Aoba, Sendai 980, Japan.
[3] Department of Astrophysics, Nagoya University, Chikusa-ku, Nagoya 464-01, Japan.
[4] Department of Physics, University of Tokyo, Bunkyo-ku, Tokyo 113, Japan.
[5] Department of Physics, Tokyo Metropolitan University, Hachioji, Tokyo 192-0, Japan.
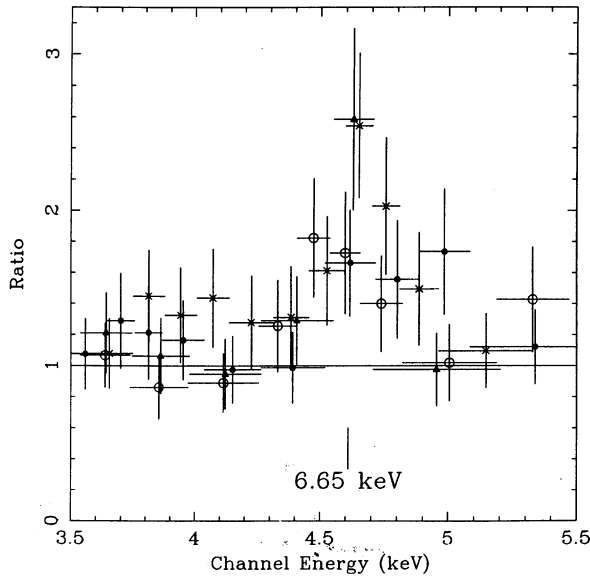[6] ISAS, 3-1-1 Yoshinodai, Sagamihara, Kanagawa 229, Japan.

FIG. 1.—Ratio of data to model in the vicinity of the redshifted iron line. The model fitted to the data consisted of a power law with excess absorption and a Gaussian line with the parameters allowed to differ between detectors (for best-fit values, see Table 1). The normalization of the Gaussian component was set to zero before the figure was plotted. Open circles denote GIS2; crosses, GIS3; filled diamonds, SIS0; and filled triangles, SIS1 data, respectively.

redshifted energy of that of cold iron (6.4 keV), with an upper limit to the equivalent width (in our frame) of 47 eV. The rest frame equivalent width of the helium-like iron line is 444^{+120}_{-173} eV. The mean, unabsorbed luminosity in the rest frame 0.5–10 keV band is 1.87×10^{45} ergs s^{-1} (we assume throughout that $H_0 = 50$ km s^{-1} Mpc^{-1}, $q_0 = 0.5$).

We have searched for other features in the spectra (Fig. 3) and find, for instance, no evidence for any strong Fe L emission (EW < 60 eV) at a rest frame energy above 0.9 keV. The limits on the equivalent width of any Si or S lines are ~ 10–20 eV.

The inclusion of a thermal spectrum characteristic of intracluster gas improves the quality of the fit by an insignificant amount ($\Delta\chi^2 \sim 2$, with abundance $Z \sim 0.3 \, Z_\odot$). The best-fit 2–10 keV luminosity of such gas is $\sim 3 \times 10^{44}$ ergs s^{-1} at a gas temperature above 2.5 keV. The maximum luminosity (at the 90% confidence level) that a 5 keV gas can have is 4.5×10^{44}

TABLE 1

SPECTRAL RESULTS

Detector	N_H[a] $(10^{22}$ cm$^{-2})$	Γ	E_K (keV)	EW[b] (eV)	χ^2/bins
GIS2......	1.13 ± 0.4	2.33 ± 0.2	6.54 ± 0.20	407 ± 200	117/133
GIS3......	0.51 ± 0.3	1.91 ± 0.2	6.64 ± 0.15	346 ± 170	158/135
SIS0	0.36 ± 0.1	2.12 ± 0.1	$6.74^{+0.6}_{-0.1}$	242 ± 160	137/122
SIS1	0.25 ± 0.1	2.09 ± 0.1	6.68 ± 0.1	470^{+7800}_{-300}	83/107
All[c]	0.24 ± 0.06	1.96 ± 0.06	6.67 ± 0.06	308^{+90}_{-120}	581/497

NOTE.—The quoted uncertainties are at the 90% confidence level for one interesting parameter.

[a] N_H is the excess intrinsic column density at $z = 0.442$. Galactic absorption from a column density of 1.6×10^{20} cm^{-2} is also included in the fits. The high value for N_H obtained for GIS2 is entirely due to the channels below 1.15 keV (see Fig. 3).

[b] The equivalent width of the iron line is as measured in our frame.

[c] For the last row, the parameter values, including the normalizations, are the same for all detectors.
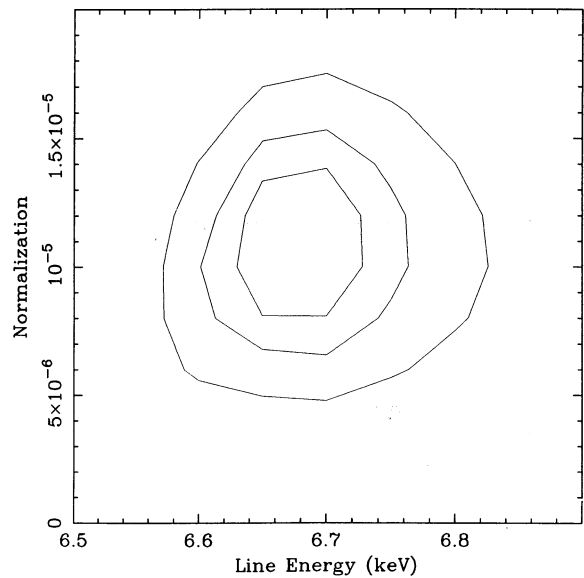
ergs s^{-1} or about 25% of the total luminosity. If the iron line were solely due to the thermal component, the abundance of that gas would be implausibly high, $Z \sim Z_\odot$ (observed values for such luminous clusters are $Z < 0.5 \, Z_\odot$; Yamashita 1992).

3. DISCUSSION

The X-ray emission from P09104+4109 is pointlike at the resolution of *ASCA* and is characterized by a power-law spectrum with some intrinsic absorption and a strong emission line from helium-like iron. The spectral index of $\Gamma = 1.96 \pm 0.06$ is remarkably similar to that observed with *Ginga*, after accounting for reflection effects, from nearby Seyfert 1 galaxies ($\Gamma = 1.95 \pm 0.05$; Nandra & Pounds 1994). The luminosity

FIG. 2.—Confidence contours (68%, 90%, and 99% for two interesting parameters) for the iron K-line energy and normalization.
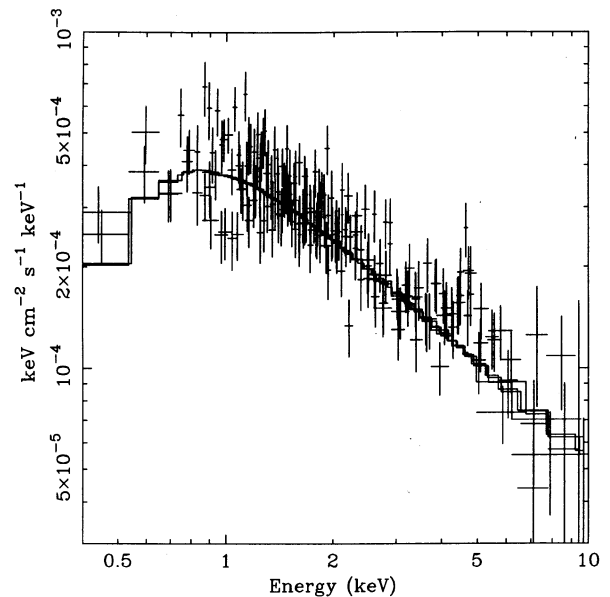

FIG. 3.—Unfolded energy spectrum for IRAS P09104+4109. The only significant feature is the iron line redshifted to 4.6 keV.

observed from P09104+4109 is, however, much larger than that of Seyfert galaxies.

The strong iron line is similar to those seen in the X-ray spectra of Seyfert 2 galaxies such as NGC 1068 (Marshall et al. 1993; Ueno et al. 1994) which are interpreted as the scattered continuum of an obscured nucleus. The iron line is produced in the scattering region by fluorescence (Krolik & Kallman 1987) and resonance scattering (Band et al. 1989). Indeed, those are the only plausible ways to obtain such a strong iron line and a (relatively) unabsorbed continuum. The observation of the strong iron line confirms that we are seeing scattered X-rays from a hidden quasar.

There are several differences between our spectrum of P09104+4109 and that of lower luminosity Seyfert 2 galaxies. The first is the energy of the iron line which indicates that the iron is highly ionized. In the case of NGC 1068, the observed line is either broad or a blend of the (dominant) neutral, He-like and H-like lines (Marshall et al. 1993). This is explained by much of the scattering material in this case being only warm (a few $\times 10^5$ K). For P09104+4109, either all the material is much hotter or any warm material is out of our line of sight. Another difference is in the continuum, which in NGC 1068 consists of a combination of steep (probably extended; Wilson et al. 1992) and flat components. This last component could be flat due to the absorbing effect of the colder scattering medium, compared with P09104+4109 the continuum of which is well fitted by a single power law.

A consistent model of the scattering process in P09104+4109 is obtained if we assume that the scattering medium is the intracluster gas surrounding the central host galaxy of the quasar. The Thomson depth in the inner few kpc of such gas can exceed 1% if the galaxy is surrounded by a cooling flow (Fabian 1989; White et al. 1994). The hot intracluster gas then electron-scatters the quasar continuum and produces an iron emission line by both recombination following K-shell ionization and by resonantly scattering continuum photons of the appropriate energy.

As shown by Band et al. (1990), this last process can dominate Fe K line production in these circumstances. In the case of Fe XXV, the equivalent width of the line from resonantly scattered continuum is as large as $4Z$ keV (using eq. [7] of Band et al. 1990 with the oscillator strength $f_{lu} = 0.79$ and the effective fluorescent yield in this case being unity), where Z is the abundance of iron Fe XXV relative to hydrogen atoms in units of 3×10^{-5} ($Z \approx Z_\odot$ if all the iron is Fe XXV). This process leads to the production of the resonance line at 6.70 keV. The large resultant equivalent width here means that the line is easily saturated and is only relevant for very small Thomson depths. The process does not create line photons, so the equivalent width of the observed line cannot exceed the ratio of the width of the line to the continuum scattering fraction. K-shell ionization of Fe XXV and Fe XXIV can both lead to a line from Fe XXV, the first through recombination and the second by deexcitation of the ion. From equation (8) of Band et al. (1990; see also Krolik & Kallman 1987), these processes each give an equivalent width of $0.6Z$ keV, where Z is here the abundance of the relevant ionization stage, and the line is the intercombination one at 6.67 keV. With our data, we are unable to distinguish between lines only 30 eV apart.

Since the abundance of iron in clusters is typically 0.2–0.5 in these units (Yamashita 1992), the equivalent width can be as large as 1000–2500 eV, which is much larger than we observe. Indeed, the iron abundance in the scattering medium must be

subsolar in order that the line is as *weak* as we observe. Since, however, the dominant resonant line can be both saturated and trapped with consequent multiple scattering, the observed equivalent width can thereby be much reduced, especially if there is cold matter present which can absorb trapped photons by the photoelectric effect. In a cluster cooling flow model, the excess intrinsic absorption could be similar to that discovered (White et al. 1991), and seen with ASCA (Fabian et al. 1994), around nearby clusters with cooling flows. Alternatively, the photons at the energy of the resonance line may be trapped at small, unobserved, radii near the source and absorbed by the dust-emitting torus. The lack of strong iron L emission can similarly be due to those lines being trapped and self-absorbed (Band et al. 1990). Further understanding of the line structure and strength must await more detailed observations of the velocity, ionization state, and depth of the scattering material.

Kleinmann et al. (1988) argue from a comparison of the $H\beta$ and IR luminosities that about 2% of the radiation from the central object is scattered into our line of sight. The argument assumes that the same ultraviolet luminosity is incident on the dust as incident on the dust-free, $H\beta$-emitting region. The dust covering factor argument does, however, rely on the $H\beta$-emitting region completely covering the holes in the dust screen. Since in most quasars the narrow-line–emitting region, which this $H\beta$-emitting region presumably is, can have a covering fraction of only 1% or less, the above dust covering factor is a lower limit, perhaps by an order of magnitude.

We can obtain a separate estimate of the dust-covering fraction by noting that the observed, scattered, X-ray luminosity, L_{XO} is related to the emitted luminosity (assumed isotropic), L_X, through the Thomson optical depth, τ_T and the solid angle subtended at the source not covered by dust, Ω:

$$L_{XO} = \frac{\Omega}{4\pi} \tau_T L_X .$$

The infrared luminosity, which is due to the fraction of the bolometric power, L_{Bol}, absorbed by the dust is

$$L_{IR} = \left(1 - \frac{\Omega}{4\pi}\right) L_{Bol} .$$

We observe for P09104+4109 that $L_{IR}/L_{XO} \approx 50$.

Now for many quasars the emitted X-ray power is a fraction $f \sim 0.1$ of the bolometric power:

$$\frac{L_X}{L_{Bol}} = 0.1 f_{0.1} .$$

Thus

$$L_{Bol} = 200 L_{XO} \frac{(1 + 0.25 f_{0.1} \tau_{0.05})}{\tau_{0.05} f_{0.1}} ,$$

where $\tau_T = 0.05 \tau_{0.05}$, so that

$$L_{Bol} \approx 5 \times 10^{47} \text{ ergs s}^{-1} ,$$

if $f_{0.1}$ and $\tau_{0.05}$ are both about unity.

In this approach, the dust-covering factor and thus the fraction of the total luminosity emitted in the IR is about 20% and IRAS P09104+4109 therefore becomes one of the most luminous objects in the universe. The opening angle of the cone, in the picture of Hines & Wills (1993), is about 70° (i.e., the solution to their polarization equation which they dismissed). In order that there is no evidence for the direct continuum in our

X-ray spectra, The Thomson optical depth in the absorbing torus must exceed unity.

We note briefly that τ_T cannot be large, as required if the dust covering factor is high, or there would be too much X-ray bremsstrahlung emission from the scattering region; $L_{br} \sim 7 \times 10^{44} \tau_{0.05}^2 T_X^{1/2} R$ ergs s^{-1}, where the region has a radius of R kpc and the temperature $T_X = 3 \times 10^7$ K. The size cannot be made much smaller than a kpc or the iron more highly ionized (the ionization parameter $\xi = L/nR^2 \sim 440 L_{47} \tau_{0.05}^{-1} R^{-1}$: iron is significantly hydrogen-like if $\xi > 1000$; Hatchett, Buff, & McCray 1976). Our limits on a thermal component and on the ionization state of the iron together imply that $\tau < 0.1$ and $R > 250$ pc (note that the limits are not improved by assuming that the region is aspherical). As noted earlier, there are strong similarities (cluster environment and weak radio source) between IRAS P09104+4109 and H1821+643 (Hines & Wills 1993), which has $L_X \sim 0.1 L_{Bol}$ (Kitt et al. 1991; Kolman et al. 1993), thereby justifying a value of $f \sim 0.1$.

4. SUMMARY

ASCA observations of IRAS P09104+4109 show an X-ray luminosity of about $L_{XO} = 2 \times 10^{45}$ ergs s^{-1} and a strong helium-like iron line from a pointlike source. The X-ray flux is scattered into our line of sight by highly ionized gas which is plausibly the innermost, dense cooling part of the intracluster medium surrounding the host galaxy. If the central engine emits isotropically, then a comparison of the IR dust and X-ray luminosities indicates that IRAS P09104+4109 is one of the most luminous objects in the universe, with $L_{Bol} = 5 \times 10^{47}$ ergs s^{-1}.

Its directly viewed counterpart is H1821+643, to which it bears a relation similar to that of Seyfert 2 to Seyfert 1 galaxies. Unlike the low-luminosity Seyfert galaxies which are generally found in spiral galaxies, IRAS P09104+4109 and H1821+643 are both in giant elliptical galaxies. Nevertheless, they demonstrate that there may be a large population of obscured quasars of which IRAS P09104+4109 is most extreme and nearest example.

Future X-ray observations with *ROSAT*, *AXAF*, and later generation instruments should spatially resolve the cluster and scattered X-ray components and measure the expected high polarization of the scattered X-rays. High-resolution X-ray spectroscopy with *ASTRO E* should enable progress to be made on the line production and scattering mechanisms.

REFERENCES

Antonucci, R. R. 1993, ARA&A, 31, 473
Band, D. L., Klein, R. I., Castor, J. I., & Nash, J. K. 1990, ApJ, 362, 90
Cutri, R. M., Huchra, J. P., Low, F. J., Brown, R. L., & Vanden Bout, P. A. 1994, ApJ, 424, L65
Fabian, A. C. 1989, MNRAS, 238, 41P
Fabian, A. C., Arnaud, K. A., Bautz, M. W., & Tawara, Y. 1994, ApJ, 436, L63
Furuzawa, A., et al. 1994, in New Horizons in X-Ray Astronomy, ed. F. Makino (New York: Universal Academy), in press
Hatchett, S., Buff, J., & McCray, R. 1976, ApJ, 206, 847
Hines, D. C., & Wills, B. J. 1993, ApJ, 415, 82
Kii, T., et al. 1991, ApJ, 367, 455
Kleinmann, S. G., Hamilton, D., Keel, W. C., Wynn-Williams, C. G., Eales, S. A., Becklin, E. E., & Kuntz, K. D. 1988, ApJ, 328, 161
Kolman, M., Halpern, J. P., Shrader, C. R., Filippenko, A. V., Fink, H. H., & Schaeidt, S. G. 1993, ApJ, 402, 514
Krolik, J. K., & Kallman, T. R. 1987, ApJ, 320, L5

Lawrence, A., et al. 1993, MNRAS, 260, 28
Marshall, F. E., et al. 1993, ApJ, 405, 168
Nandra, K., & Pounds, K. A. 1994, MNRAS, 268, 405
Rowan-Robinson, M., et al. 1991, Nature, 351, 719
Tanaka, Y., Inoue, H., & Holt, S. S. 1994, PASJ, 46, L37
Ueno, S., Mushotzky, R. F., Koyama, K., Iwasawa, K., Awaki, H., & Hayashi, I. 1994, PASJ, 46, L71
White, D. A., Fabian, A. C., Johnstone, R. M., Mushotzky, R. F., & Arnaud, K. A. 1991, MNRAS, 252, 72
White, D. A., et al. 1994, MNRAS, 269, 589
Wilson, A. S., Elvis, M., Lawrence, A., & Bland-Hawthorn, J. 1992, ApJ, 391, L75
Yamashita, K. 1992, in Frontiers of X-ray Astronomy, ed. Y. Tanaka & K. Koyama (Tokyo: Universal Academy), 475
Yaqoob, T., et al. 1994, PASJ, 46, L145